Cancer Research

Antitumor Activity of Hyaluronic Acid Synthesis Inhibitor 4-Methylumbelliferone in Prostate Cancer Cells

Vinata B. Lokeshwar[1,2,3], Luis E. Lopez[1], Daniel Munoz[1], Andrew Chi[1], Samir P. Shirodkar[1], Soum D. Lokeshwar[1,3], Diogo O. Escudero[2], Neetika Dhir[1,*], and Norman Altman[4]

Abstract

4-Methylumbelliferone (4-MU) is a hyaluronic acid (HA) synthesis inhibitor with anticancer properties; the mechanism of its anticancer effects is unknown. We evaluated the effects of 4-MU on prostate cancer cells. 4-MU inhibited proliferation, motility, and invasion of DU145, PC3-ML, LNCaP, C4-2B, and/or LAPC-4 cells. At IC_{50} for HA synthesis (0.4 mmol/L), 4-MU induced >3-fold apoptosis in prostate cancer cells, which could be prevented by the addition of HA. 4-MU induced caspase-8, caspase-9, and caspase-3 activation, PARP cleavage, upregulation of Fas-L, Fas, FADD and DR4, and downregulation of bcl-2, phosphorylated bad, bcl-XL, phosphorylated Akt, phosphorylated IKB, phosphorylated ErbB2, and phosphorylated epidermal growth factor receptor. At IC_{50}, 4-MU also caused >90% inhibition of NF-κB reporter activity, which was prevented partially by the addition of HA. With the exception of caveolin-1, HA reversed the 4-MU–induced downregulation of HA receptors (CD44 and RHAMM), matrix-degrading enzymes (MMP-2 and MMP-9), interleukin-8, and chemokine receptors (CXCR1, CXCR4, and CXCR7) at the protein and mRNA levels. Expression of myristoylated-Akt rescued 4-MU–induced apoptosis and inhibition of cell growth and interleukin-8, RHAMM, HAS2, CD44, and MMP-9 expression. Oral administration of 4-MU significantly decreased PC3-ML tumor growth (>3-fold) when treatment was started either on the day of tumor cell injection or after the tumors became palpable, without organ toxicity, changes in serum chemistry, or body weight. Tumors from 4-MU–treated animals showed reduced microvessel density (~3-fold) and HA expression but increased terminal deoxynucleotidyl transferase–mediated dUTP nick end labeling–positive cells and expression of apoptosis-related molecules. Therefore, the anticancer effects of 4-MU, an orally bioavailable and relatively nontoxic agent, are primarily mediated by inhibition of HA signaling. *Cancer Res; 70(7); 2613–23. ©2010 AACR.*

Introduction

Hyaluronic acid is a nonsulfated glycosaminoglycan made up of D-glucuronic acid and *N*-acetyl-D-glucosamine. Hyaluronic acid (HA) expression is elevated in a variety of tumors (1). In prostate tumor tissues, elevated HA levels are contributed by both tumor-associated stroma and tumor cells, and together with HYAL-1 hyaluronidase, predict disease progression (2–6). HA regulates several cellular functions (7–9). In the human genome there are three HA synthase (HAS) genes, *HAS1*, *HAS2*, and *HAS3*, each of the HAS synthesizes HA of different molecular mass (10–12). Silencing HAS genes in tumor cells inhibits cell proliferation, invasion, and motility *in vitro* and tumor growth and metastasis *in vivo* (11–17). For example, knockdown of HAS1 expression induces Fas-mediated apoptosis and inhibits invasion *in vitro* and causes inhibition of tumor growth, infiltration, and angiogenesis in xenografts (16). In prostate cancer cells, HA synthase expression requires HYAL-1 hyaluronidase to promote tumor growth, metastasis, and angiogenesis (13, 14). These results are consistent with our observations that HYAL-1 is a molecular determinant of tumor growth, invasion, and angiogenesis (18, 19) and suggest that a finely regulated cellular HA-hyaluronidase system promotes tumor growth and progression.

The cellular effects of HA are mediated through HA receptors, CD44 and RHAMM. CD44-HA interaction induces the activation of receptor tyrosine kinases (20–22). HAS1 knockdown inhibits ErbB2 activation and transcriptionally downregulates CD44 (16). HA-induced CD44-epidermal growth factor receptor (EGFR) interaction and EGFR activation promotes cellular motility through Akt signaling and increased expression of MMP-2/MMP-9 (22–25). HA also induces interleukin-8 (IL-8) and stromal-derived factor-1 (SDF-1) receptor (CXCR4) expression through NF-κB activation (25–31). IL-8 expression promotes tumor growth,

Authors' Affiliations: Departments of [1]Urology, [2]Cell Biology and Anatomy, [3]Sylvester Comprehensive Cancer Center, and [4]Department of Pathology, University of Miami Miller School of Medicine, Miami, Florida

Note: Supplementary data for this article are available at Cancer Research Online (http://cancerres.aacrjournals.org/).

*We dedicate this article to our colleague, Ms. Neetika Dhir, whose untimely death saddened us all.

Corresponding Author: Vinata B. Lokeshwar, Division of Urology Research, Department of Urology (M-800), University of Miami Miller School of Medicine, P.O. Box 016960, Miami, FL 33101. Phone: 305-243-6321; Fax: 305-243-6893; E-mail: vlokeshw@med.miami.edu.

doi: 10.1158/0008-5472.CAN-09-3185

angiogenesis, and androgen-independent growth of prostate cancer cells (31). HA-RHAMM interaction also induces intracellular signaling (32). Therefore, inhibition of HA synthesis in tumor cells should help control tumor growth and progression.

4-Methylumbelliferone (4-MU; 7-hydroxy-4-methylcoumarin) is a HA synthesis inhibitor with choleretic and antispasmodic properties (Heparvit). In mammalian cells, HA is synthesized by HAS, using UDP-glucuronic acid (UGA) and UDP-*N*-acetyl-D-glucosamine precursors. UGA is synthesized when UGA-transferase transfers UDP to glucuronic acid. In cells treated with 4-MU, UGA-transferase transfers glucuronic acid onto 4-MU. This depletes the intracellular pool of UGA, resulting in the inhibition of HA synthesis (33–37). 4-MU also downregulates HAS2 and HAS3 expression (38). Oral administration of 4-MU (600 mg/kg/d) reduces metastases by 64% in the B16 melanoma model (34). Currently, intracellular signaling events involved in the antitumor effects of 4-MU are unknown. In this study, we evaluated the antitumor activity of 4-MU in prostate cancer cells and in a xenograft model.

Materials and Methods

Cell culture. Prostate cancer cells LNCaP, DU145, and PC3-ML were cultured in RPMI 1640 + 10% fetal bovine serum + gentamicin (18, 31). LAPC-4 cells were maintained in Iscove's medium with 7.5% fetal bovine serum and 1 nmol/L of dihydrotestosterone (31). C4-2B cells were cultured in T-Medium + 10% fetal bovine serum + gentamicin.

Reagents. 4-MU was purchased from Sigma-Aldrich. Hyaluronic acid sodium salt was purchased from MBL and Lifecore Biomedical. All of the antibodies and constructs used in this study are described in the Supplementary Information.

HA ELISA-like assay. Twenty-four–hour cultures of PC3-ML and DU145 cells (10^5 cells/well; 12-well plates) were treated with 4-MU, coumerin, or 4-hydroxycoumerin (0–0.8 mmol/L) for 36 h. Conditioned media were analyzed by HA ELISA-like assays and HA levels were normalized to cell number (6).

Cell proliferation and apoptosis. Prostate cancer cells (2.0×10^4 cells/well; 24-well plates) cultured in growth medium were exposed to 4-MU (0–0.6 mmol/L) and counted after 72 h. Alternatively, cells (1.5×10^4) were exposed to 4-MU (0.4 mmol/L) and counted every 24 h. For the apoptosis assay, cells plated on 24-well plates were exposed to 4-MU (0–0.6 mmol/L). Following 24 or 48 h of incubation, apoptosis was analyzed using the Cell Death ELISA Plus kit (Roche Diagnostics). The apoptosis index was calculated as $OD_{450\ nm}$ per 20,000 cells. In some experiments, 50 μg/mL of HA was introduced to the wells at the time of 4-MU addition.

Motility and invasion assays. Matrigel invasion assay was carried out as described previously (16, 18, 19), except that 4-MU was added in both chambers of the Transwell; for details, please see Supplementary Information. To neutralize the effect of 4-MU on cell growth, percentage of invasion or motility was calculated as [OD bottom chamber / OD (top + bottom chambers)] ×100.

Immunoblot analyses and time course. Prostate cancer cells were exposed to 4-MU (0–0.6 mmol/L) for 24 to 48 h. For time course experiments, 14-h cultures of PC3-ML were exposed to 4-MU (0.4 mmol/L) for 4, 8, 12, 18, and 24 h. The cell lysates (~20 μg/mL) were analyzed by immunoblotting using specific antibodies. In some wells, 50 μg/mL of HA was introduced at the time of 4-MU addition. The intensity of each protein band, following chemiluminescence, was determined using Kodak image analysis software.

Real-time reverse transcription-PCR assays. PC3-ML cells were treated with 4-MU ± HA (50 μg/mL) for 24 to 48 h; HA was added at the same time as 4-MU. Quantitative-PCR (Q-PCR) was performed using the iQ SYBR Green Supermix (Bio-Rad) and the primers described in Supplementary Table S1 (16). The mRNA levels were normalized to β-actin. In some experiments, 4-MU–treated cells were exposed to actinomycin D (10 μg/mL) and the rate of mRNA degradation was determined by Q-PCR. Q-PCR was also performed 72 h after transfecting PC3-ML cells with (*a*) either CD44 short interfering RNA (siRNA), RHAMM siRNA, (*b*) both CD44 and RHAMM siRNAs (50 nmol/L each), or (*c*) control nontargeting siRNA (Dharmacon; ref. 39).

Transient transfection. PC3-ML cells were transiently cotransfected with pNF-κÂ-luc and pGL4.74[*hRluc*/TK] plasmids. Eight hours following transfection, the cells were exposed to 4-MU (0.4 mmol/L) in the presence or absence of 50 μg/mL of HA. Following 24 h of incubation, the firefly luciferase and Renilla luciferase activities were assayed (40).

PC3-ML cells were also transiently transfected with a myr-Akt plasmid and then treated with 4-MU (0.4 mmol/L). Cell growth, apoptosis, gene expression (Q-PCR), and NF-κB reporter assays were conducted after 48 h. For details, please see Supplementary Information.

Tumor xenografts. PC3-ML cell suspension (2×10^6 cells/0.1 mL) was mixed 1:1 with Matrigel and implanted subcutaneously in the dorsal flank of 5- to 6-month-old athymic mice. There were 10 mice per treatment group. The mice were gavaged twice daily with vehicle (PBS) or 4-MU (225 or 450 mg/kg). The treatment began either on the day of injection or on day 7 when the tumors became palpable. Tumor volume was measured twice weekly (16, 18). Animals were euthanized when tumor volume in the control animals exceeded 0.5 cc. A portion of each tumor was either flash-frozen for preparing tumor extracts or fixed for immunohistochemistry [to localize HA and microvessels or terminal deoxynucleotidyl transferase–mediated dUTP nick end labeling (TUNEL)-positive cells; refs. 16, 18, 19, 31, 40]. For details on tumor extract preparation, determination of microvessel density (MVD) and the TUNEL assay, please see Supplementary Section. Serum chemistry was performed by the Division of Veterinary Resources, University of Miami. Lung, kidney, liver, seminal vesicles, prostate, and testes were fixed and histology was performed by the Division of Veterinary Resources.

Results

4-MU inhibited HA synthesis and cell proliferation in prostate cancer cells. PC3-ML cells secrete ~4- to 5-fold

higher HA levels when compared with DU145 cells (6). We therefore measured the effect of 4-MU on HA synthesis in PC3-ML and DU145 cells. As shown in Fig. 1A, 4-MU inhibited HA synthesis in both cell lines (IC_{50} ~0.4 mmol/L). In contrast, coumerin or 4-hydroxycoumerin did not inhibit HA synthesis (Fig. 1A).

The effect of 4-MU on cell growth is shown in Fig. 1B. After 72 hours of treatment, 4-MU inhibited the growth of all five prostate cancer cell lines (IC_{50}, 0.2–0.4 mmol/L). At ≥IC_{50}, the differences in cell numbers between untreated and 4-MU–treated samples were statistically significant ($P < 0.001$; unpaired t test). The presence of HA during incubation with 4-MU prevented 4-MU–induced inhibition of PC3-ML cell growth (IC_{50} ~ 0.8 mmol/L in the presence of HA versus 0.4 mmol/L for 4-MU alone; Fig. 1B). In the presence of 4-MU, cell detachment did not exceed 10% of the total cell count. Time course experiments showed that 4-MU inhibited the growth of prostate cancer cells at each time point (Fig. 1C; $P < 0.001$; unpaired t test). 4-MU treatment also caused a change in cell morphology. As shown in Fig. 1D, within 48 hours of 4-MU treatment, PC3-ML cells became irregular in shape with projections. The addition of HA (50 μg/mL) partially prevented this change in cell morphology (data not shown).

4-MU induced apoptosis in prostate cancer cells. We next examined whether the growth inhibition by 4-MU was due to induction of apoptosis. 4-MU induced apoptosis in prostate cancer cells, in a dose-dependent manner with ≥3-fold induction of apoptosis at IC_{50} (0.4 mmol/L; Fig. 2A). As shown in Fig. 2B, 4-MU caused 2- to 3-fold induction of apoptosis in PC3-ML cells (mean apoptosis index: untreated, 0.096; 0.2 mmol/L, 0.22; 0.4 mmol/L, 0.3; $P < 0.001$; Bonferroni multiple comparison test). However, the addition of HA prevented this effect (mean apoptosis index: 0.2 mmol/L 4-MU + HA, 0.1; 0.4 mmol/L 4-MU + HA, 0.13; $P > 0.05$; Bonferroni multiple comparison test). These results show that the effect of 4-MU on cell growth and apoptosis was due to inhibition of HA synthesis.

As shown in Fig. 2C, in PC3-ML and LAPC-4 cells, 4-MU induced the activation of proapoptotic effectors, caspase-8, caspase-9, and caspase-3 (2- to 4-fold) and PARP cleavage. Figure 2D shows that 4-MU induced the upregulation of Fas-L, Fas, FADD, and DR4 and bid cleavage (p15bid); at the 0.4 mmol/L concentration, there was 1.8- to 3-fold upregulation of these death-inducing signaling complex proteins. Eight hours following 4-MU treatment, there was an upregulation of Fas-L, Fas, and DR4, with a maximal increase occurring by 12 hours (Fig. 2D). 4-MU also caused a decrease in bcl-2 (>4-fold), bcl-XL (<2-fold), and phosphorylated bad (>2-fold) levels. The addition of HA during 4-MU treatment prevented the upregulation or downregulation of

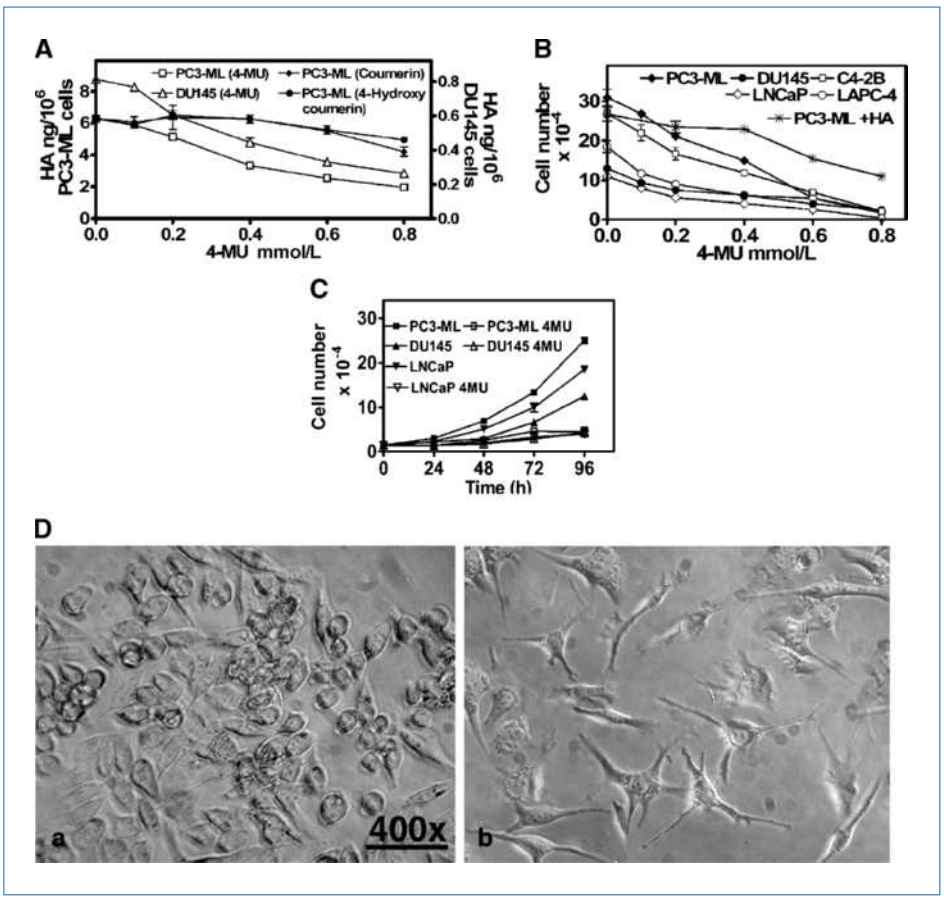

Figure 1. Effect of 4-MU on HA synthesis and cell proliferation. A, measurement of HA levels by HA ELISA-like assay. Points, mean; bars, SEM (from three experiments). B and C, cell counting data after 72 h of treatment with 4-MU (B). In some cases, PC3-ML cells were treated with 4-MU plus 50 μg/mL of HA and counted after 72 h (PC3-ML + HA graph). Prostate cancer cells were treated with 4-MU (0.4 mmol/L) and counted every 24 h (C). Points, mean; bars, SD (triplicate in two experiments). D, light microscopy of PC3-ML cells either untreated (a) or treated with 4-MU (0.4 mmol/L; b) for 48 h. Magnification, ×400.

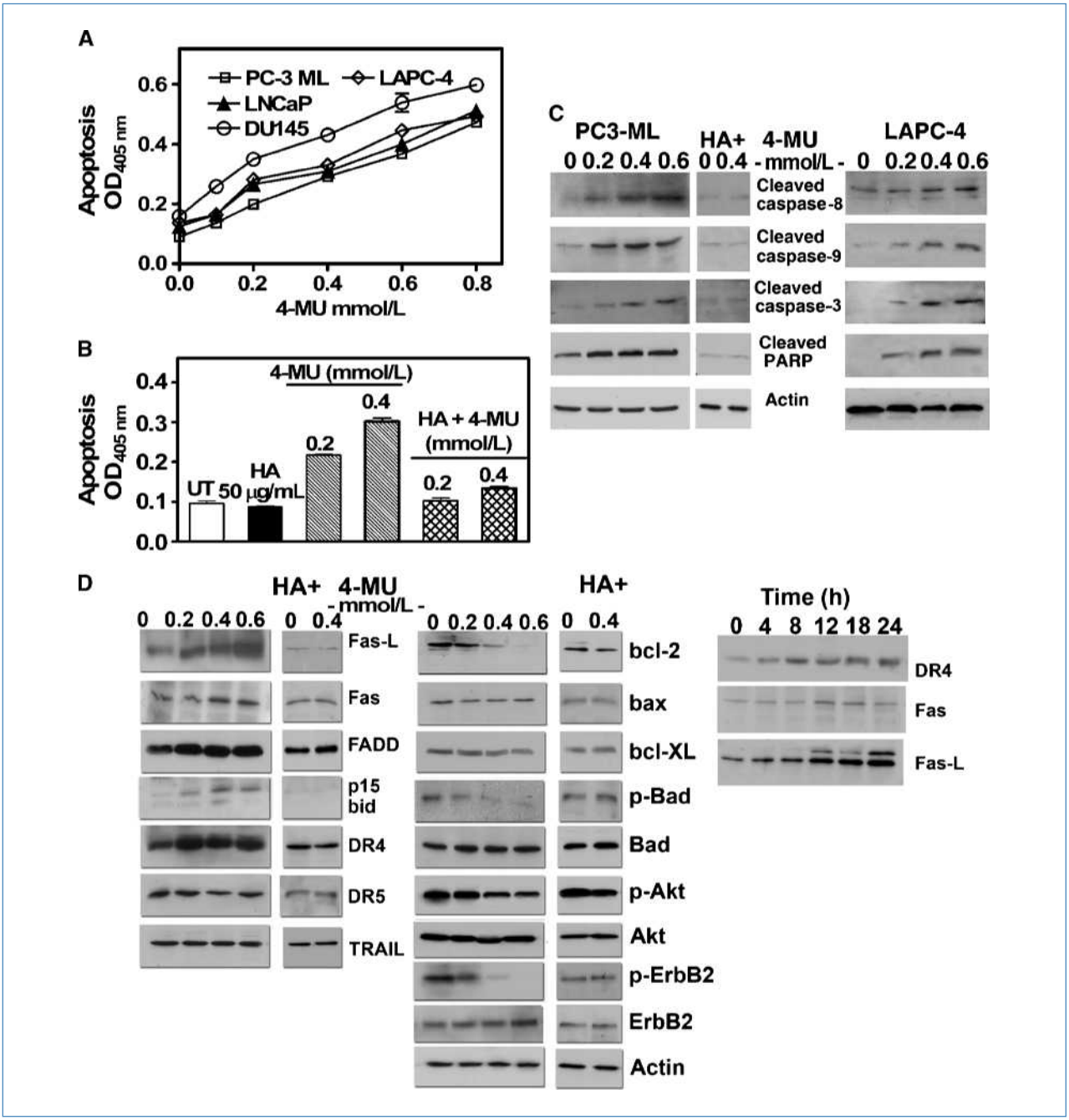

Figure 2. Effect of 4-MU on apoptosis. A, measurement of apoptosis in cells treated with 4-MU for 48 h. Points, mean; bars, SD. B, measurement of apoptosis in PC3-ML cells treated with 4-MU ± HA (50 µg/mL) for 48 h. Columns, mean; bars, SD. C and D, PC3-ML cells, treated with 4-MU, were subjected to immunoblot analyses for apoptosis-related proteins. Subpanel in D, immunoblot analyses of Fas-L, Fas, and DR4 in PC3-ML cells were treated with 4-MU (0.4 mmol/L) for the indicated time periods.

each of the signaling molecules in the apoptosis cascade (Fig. 2C and D). These results show that 4-MU decreased cell survival mainly by inducing the extrinsic pathway of apoptosis.

HA is known to induce ErbB2 and Akt activation; Akt activation induces survival by phosphorylating bad at Ser136 (16, 20–22). 4-MU induced a dose-dependent decrease in phosphorylated Akt and phosphorylated ErbB2 levels (Fig. 2D). At 0.4 mmol/L concentration, the decrease was ~ 4-fold for phosphorylated ErbB2 and >2-fold for phosphorylated Akt and HA prevented the 4-MU–induced decrease in phosphorylated Akt and phosphorylated ErbB2 levels.

4-MU inhibits invasion and chemotactic motility. Because HA promotes tumor cell migration and invasion, we examined whether 4-MU inhibits the invasive potential of prostate cancer cells. As shown in Fig. 3A and B, 4-MU induced a dose-dependent decrease in the invasive activity of PC3-ML and DU145 cells. At 0.4 mmol/L concentration, the inhibition was ~67% in both cell types ($P < 0.001$; Bonferroni multiple comparison test). However, in the presence of HA, 4-MU caused only 15% to 20% inhibition of invasion (Fig. 3A and B; $P > 0.05$).

4-MU also inhibited the chemotactic motility of PC3-ML and DU145 cells (Fig. 3C). At 0.4 mmol/L concentration, 4-MU caused a 55% and 43% inhibition of chemotactic motility in PC3-ML and DU145 cells, respectively ($P < 0.01$; unpaired t test). The addition of HA reduced this inhibition to 25% and 17%, respectively, for PC3-ML and DU145 cells. Because HA prevented 4-MU–induced inhibition of chemotactic motility and invasion, 4-MU, very likely, inhibits these properties by inhibiting HA synthesis.

4-MU downregulates HA receptor expression and regulators of invasion and motility. CD44-HA interaction induces matrix metalloproteinase expression (23, 24), and HAS1 and HAS2 knockdown transcriptionally downregulates CD44 (16, 17). Therefore, we examined whether 4-MU downregulates HA receptors (CD44 and/or RHAMM), HA synthases, and/or MMP-2 and MMP-9 levels. Consistent with our previous findings (41), PC3-ML cells express the 90 kDa standard form of CD44 (CD44s; Fig. 3D). Furthermore, 4-MU caused a dose-dependent decrease in CD44, RHAMM, HAS2, MMP-2, and MMP-9 levels (2- to 3-fold decrease at 0.4 mmol/L concentration). The addition of HA at the same time as 4-MU, prevented the downregulation of CD44, RHAMM, MMP-2, MMP-9, and HAS2 (Fig. 3D). Because the HAS2 siRNA downregulated

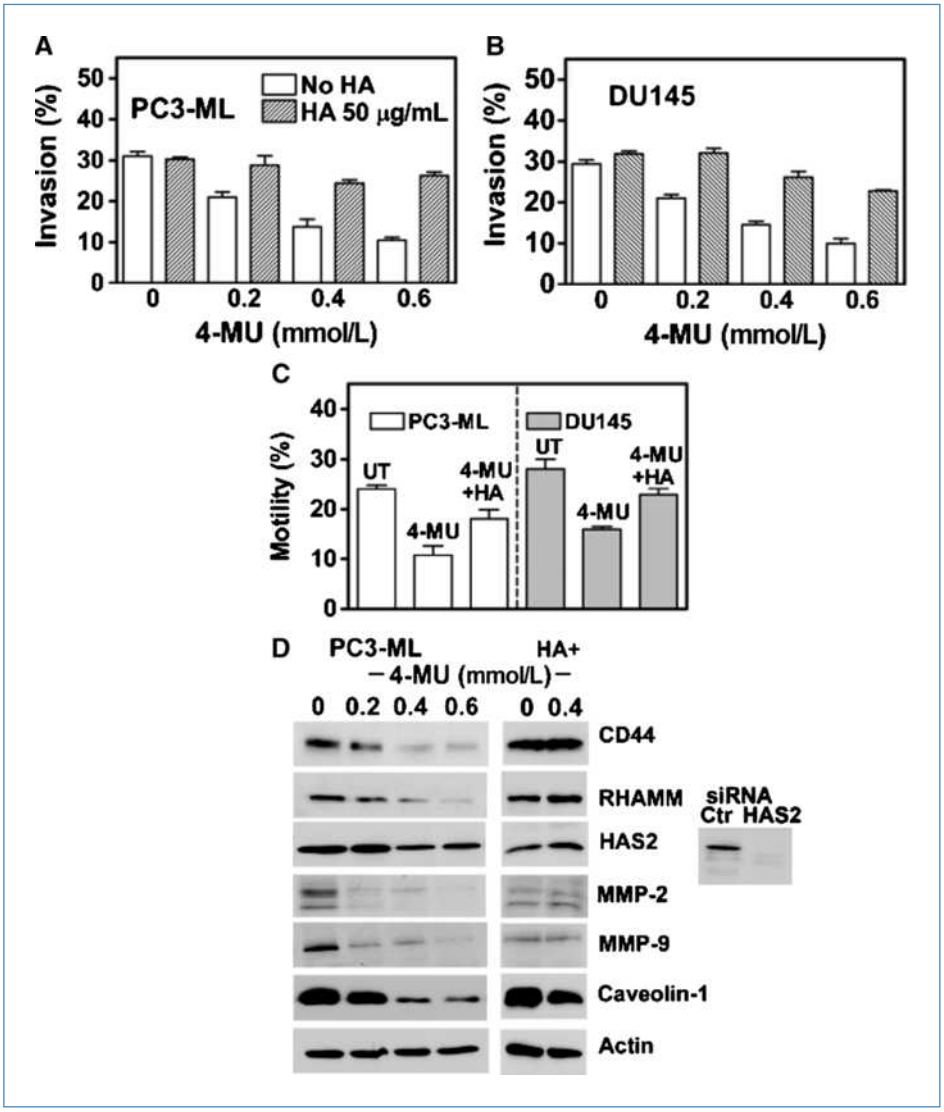

Figure 3. Effect of 4-MU on invasion and chemotactic motility. A and B, determination of invasive activity of PC3-ML (A) and DU145 (B) cells in the presence or absence of 4-MU and/or HA. Columns, mean; bars, SD (triplicate in two experiments). C, determination of chemotactic motility of PC3-ML (A) and DU145 (B) cells in the presence or absence of 4-MU and/or 50 μg/mL of HA. Columns, mean; bars, SD. D, PC3-ML cells treated with 4-MU were subjected to immunoblot analysis. Side panel, PC3-ML cells were transfected with control or HAS2 siRNA and subjected to immunoblot analysis using the anti-HAS2 antibody.

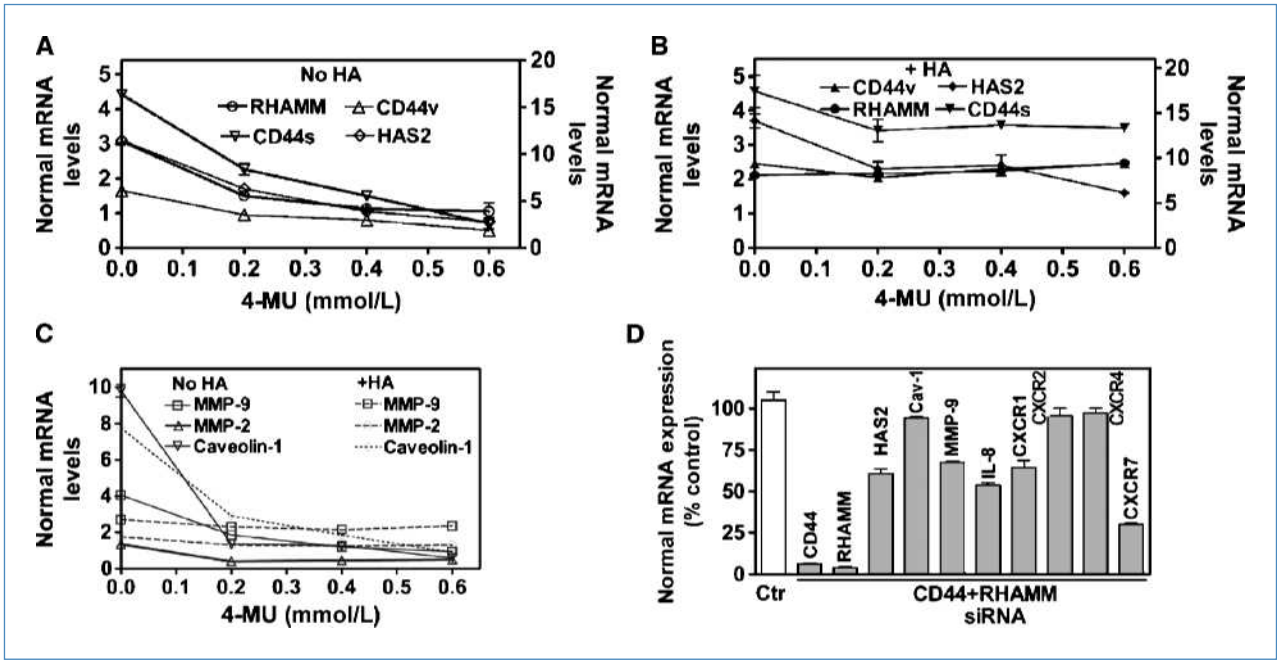

Figure 4. Effect of 4-MU and CD44-RHAMM siRNA-treated cells on gene expression. A, B, and C, PC3-ML cells were treated with 4-MU in the absence (A and C) or presence of HA (B and C) and the mRNA levels of the indicated genes were assayed by Q-PCR. D, PC3-ML cells were treated with CD44 and RHAMM siRNA and the mRNA levels were analyzed by Q-PCR.

the protein band detected by HAS2 antibody, it showed that the anti-HAS2 antibody was specific (Fig. 3D).

In prostate cancer, elevated caveolin-1 expression correlates with disease progression and promotes cell survival and angiogenesis (42). As shown in Fig. 3D, 4-MU induced ~10-fold decrease in caveolin-1 expression; however, the addition of HA did not prevent this decrease.

4-MU also induced a dose-dependent downregulation of CD44, RHAMM, MMP-2, MMP-9, and caveolin-1 mRNA levels (Fig. 4A and C). The mean CD44s mRNA levels in untreated samples (15.15 ± 0.85) were 9.2 times higher than CD44v mRNA levels (1.65 ± 0.25), confirming that PC3-ML cells mainly express the CD44s form. At the 0.4 mmol/L concentration, 4-MU decreased CD44s, CD44v, RHAMM, HAS2, MMP-2, and MMP-9 mRNA levels by 2.5- to 3-fold and caveolin-1 mRNA levels by 7.7-fold ($P < 0.001$ for each mRNA). 4-MU did not alter HAS1 and HAS3 mRNA levels (data not shown). The addition of HA completely prevented the 4-MU–induced decrease in CD44, RHAMM, HAS2, MMP-2, and MMP-9 mRNA levels (Fig. 4B) and caused a partial prevention of the decrease in HAS2 mRNA levels (no 4-MU, 3.7 ± 0.2; 0.4 mmol/L 4-MU, 2.4 ± 0.3). However, HA did not prevent the decrease in caveolin-1 levels (Fig. 4C). Comparison between the effect of 4-MU and 4-MU + HA treatments on the expression of each gene presented in Fig. 4A–C is shown in Supplementary Table S2.

The decrease in mRNA levels of the genes described above was most likely transcriptional because the mRNA degradation rates in the presence and absence of 4-MU were similar in PC3-ML cells treated with actinomycin-D (data not shown).

Because HA prevented the effect of 4-MU on gene expression, we determined whether downregulation of CD44 and/or RHAMM expression by siRNA would similarly affect the gene expression. Downregulation CD44 or RHAMM by themselves did not significantly alter MMP-2, MMP-9, or caveolin-1 mRNA levels (data not shown). However, simultaneous downregulation of CD44 and RHAMM decreased the mRNA levels of both receptors by >95% and of HAS2 and MMP-9 levels by ~35% to 40%; no downregulation of caveolin-1 mRNA was observed (Fig. 4D). The data related to the downregulation of other genes shown in the figure are discussed below.

Because 4-MU is currently the only known compound with a well characterized biochemical mechanism of inhibition of HA synthesis (35, 36), we examined whether downregulation of HAS2, CD44, RHAMM, or both CD44 and RHAMM mimics the biological effects of 4-MU. As shown in Supplementary Fig. S1A, downregulation of HAS2, CD44, RHAMM, and CD44 + RHAMM caused 68.5%, 47.7%, 57.7%, and 64% inhibition of cell growth, respectively; the decrease was statistically significant in each case ($P < 0.001$; unpaired t test). Downregulation of each of these genes induced a 1.5- to 2-fold induction of apoptosis within 48 hours (Supplementary Fig. S1B).

4-MU downregulates IL-8, IL-8 receptors, and CXCR4. HA induces EGFR and Akt activation, and upregulates IL-8 and CXCR4 through NF-κB activation (26–30). Therefore, we examined the effect of 4-MU on EGFR and Akt phosphorylation. As shown in Fig. 5A, 4-MU decreased phosphorylated EGFR and phosphorylated Akt levels with similar kinetics (~50% decrease by 8 hours), whereas the downregulation

of CD44 and RHAMM levels by 4-MU occurred at later time points (~50% in 12 hours).

Akt activates NF-κB by phosphorylating IKKα, which in turn, phosphorylates IKB, targeting it for degradation. As shown in Fig. 5A, 4-MU decreased phosphorylated IKB levels >4-fold after 12 hours of treatment, with an increase in total IKB levels at 18 and 24 hours. The addition of HA prevented 4-MU–induced decrease in phosphorylated IKB levels. The effect of 4-MU treatment on NF-κB promoter luciferase reporter activity is shown in Fig. 5B. At 0.4 mmol/L, 4-MU inhibited NF-κB reporter activity by 83% (51.8 ± 6.8 versus 8.8 ± 2.3; $P < 0.001$ unpaired t test), and HA partially prevented this inhibition (relative activity, 29.6 ± 2.0). Downregulation of CD44, RHAMM, or both receptors simultaneously, as well as downregulated NF-κB reporter activity by 54% to 70% (Fig. 5B).

We next examined the effect of 4-MU on IL-8 (CXCR1 and CXCR2) and SDF-1 (CXCR4 and CXCR7) receptors. As shown in Fig. 5A, 4-MU caused a dose decrease in CXCR1, CXCR4, and CXCR7 levels (IC_{50}, 0.4 mmol/L), with no alterations in CXCR2 levels. Furthermore, the addition of HA prevented this decrease (Fig. 5A). Q-PCR analyses showed that 4-MU decreased CXCR1, CXCR4, and CXCR7 mRNA levels by 0.4 mmol/L concentration (Fig. 5C). 4-MU also caused a dose-dependent decrease in IL-8 levels (~5-fold at 0.4 mmol/L). 4-MU did not alter SDF-1 mRNA levels (data not shown). The addition of HA completely prevented the decrease caused by 4-MU in CXCR1, CXCR4, and CXCR7 mRNA levels and partially prevented a decrease in IL-8 mRNA and IL-8 levels (from 5- to 10-fold to 2-fold; Fig. 5D). Simultaneous downregulation of both CD44 and RHAMM by siRNA also induced a 35% to 70% downregulation in CXCR1, IL-8, and CXCR7 levels, but no decrease in CXCR4 levels (Fig. 4D). Therefore, it is likely that 4-MU inhibits IL-8 and chemokine receptor expression by negatively regulating HA-HA receptor interaction.

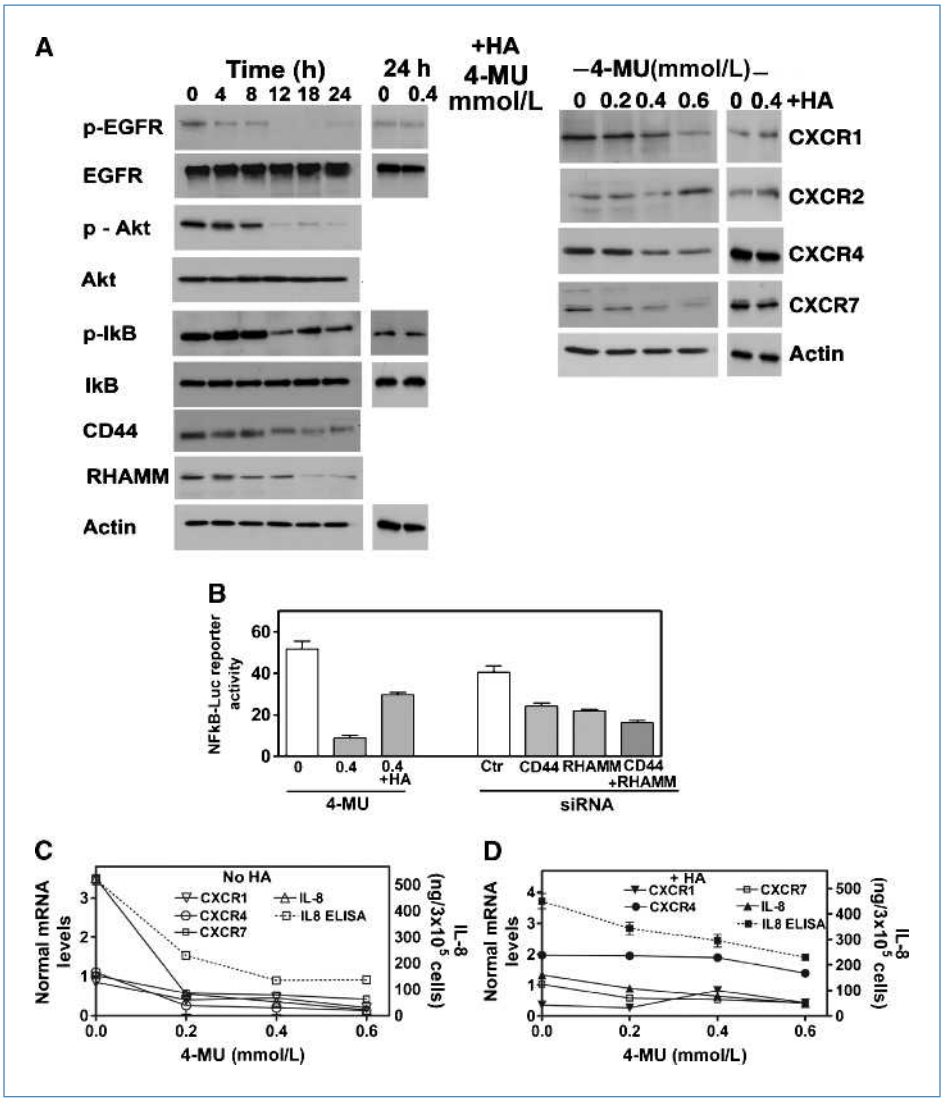

Figure 5. Analysis of HA-related signaling events in 4-MU–treated cells. A, PC3-ML cells were treated with 0.4 mmol/L of 4-MU for various time periods and subjected to immunoblot analyses (left). Immunoblot analyses of CXCR1, CXCR2, CXCR4, and CXCR7 in 4-MU–treated PC3-ML cells (right). B, PC3-ML cells cotransfected with NF-κB promoter Luciferase reporter and Renilla luciferase plasmids were treated with 4-MU (0.4 mmol/L) and/or HA (50 μg/mL; left). Luciferase activity was measured as described in Materials and Methods. NF-κB promoter Luciferase reporter activity in PC3-ML cells transfected with control, CD44, RHAMM, or CD44 and RHAMM siRNAs (right). C and D, PC3-ML cells were treated with 4-MU in the absence (C) or presence of HA (D). Following 48 h of incubation, mRNA levels were determined by Q-PCR.

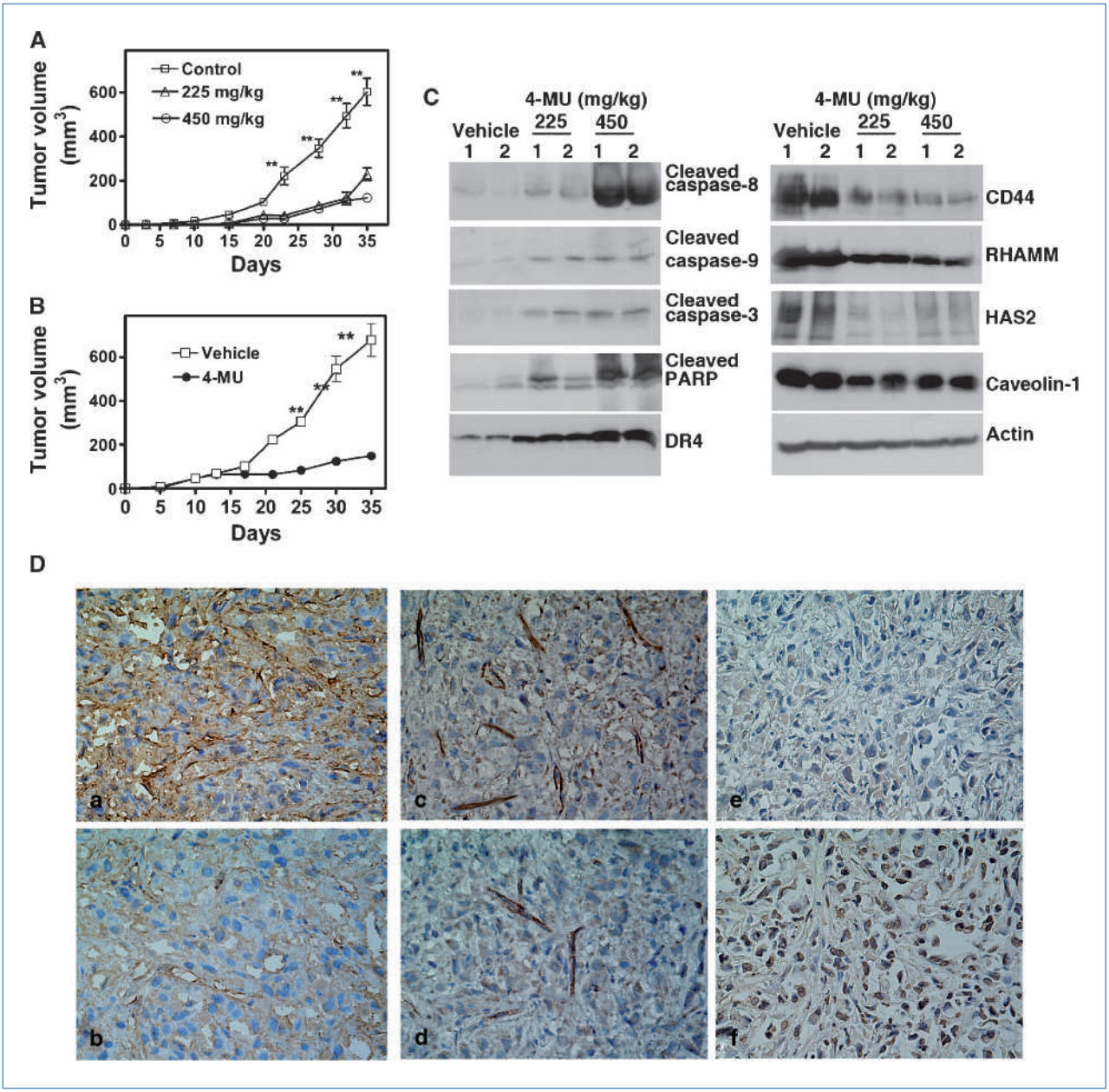

Figure 6. Effect of 4-MU on PC3-ML tumor xenografts. A and B, athymic mice implanted subcutaneously with PC3-ML cells were orally gavaged twice daily either with vehicle or 4-MU (225 or 450 mg/kg). A, treatment started on the day of the injection. B, treatment (4-MU, 450 mg/kg) started 7 d post-tumor implantation. C, immunoblot analyses of tumor tissue extracts from vehicle-treated and 4-MU–treated animals. D, HA localization and microvessel density determination by immunohistochemistry (magnification for all panels, ×400). a and b, HA staining; c and d, localization of microvessels. The area of the highest MVD from each specimen is presented here; e and f, TUNEL assay; a, c, and e, vehicle; b, d, and f, 4-MU treatment.

Effect of constitutive Akt activation on 4-MU–induced cellular effects. To understand the mechanism by which 4-MU might inhibit cell growth, gene expression, and induce apoptosis, we evaluated various effects of 4-MU in PC3-ML cells transfected with a myristoylated-Akt plasmid (m-Akt, constitutively active Akt). As shown in Supplementary Fig. S1A, m-Akt transfection increased total Akt levels by 3-fold and p-Akt levels by over 10-fold when compared with the vector control. p-Akt levels were not appreciably reduced (<2-fold) in the presence of 4-MU. Supplementary Fig. S1B, C, and D show that m-Akt expression attenuated the effect of 4-MU on cell growth, apoptosis, and NF-κB reporter activity. Expression of myr-Akt also reversed the inhibitory effect of 4-MU on IL-8, HAS2, RHAMM, CD44, and MMP-9 expression (Supplementary Fig. S1E). However, myr-Akt expression did not alter the 4-MU–induced

downregulation of caveolin-1, CXCR1, CXCR7, and CXCR4 mRNAs (data not shown).

Effect of 4-MU on tumor growth and angiogenesis. The effect of 4-MU treatment by oral gavage on PC3-ML xenografts is shown in Fig. 6A. 4-MU significantly inhibited tumor growth at both 225 and 450 mg/kg, doses ($P < 0.001$; Bonferroni's multiple comparison test). Tumor weight at necropsy in the vehicle-treated group (299.4 ± 81.5) was three times higher than in the 4-MU–treated groups (225 mg/kg: 112.9 ± 21.9; 450 mg/kg: 83 ± 16.1). Unlike coumerin, which causes loss of body weight and reduction in prostate, testis, and seminal vesicle weights (43), the 4-MU treatment (450 mg/kg) did not cause such reductions ($P > 0.05$; Supplementary Fig. S2A and B). 4-MU also did not cause gross histologic changes in prostate, testis, seminal vesicles, liver, kidney, and lung tissues (data not shown). Serum chemistry analysis showed no significant differences in blood urea nitrogen, creatinine, serum glutamic pyruvic tranaminase, and alkaline phosphatase levels from vehicle-treated and 4-MU–treated (450 mg/kg) animals ($P > 0.05$; Supplementary Table S3). Blood clotting time was also similar in both groups.

We next determined whether 4-MU delayed tumor growth if the treatment started after the tumors became palpable (7th day). As shown in Fig. 6B, 4-MU (450 mg/kg) significantly slowed tumor growth ($P < 0.001$ at each time point). Tumor weight at necropsy in the vehicle-treated group (338 ± 131) was 4-fold higher than in 4-MU–treated groups (79 ± 37.2; $P < 0.001$).

Analyses of tumor tissue extracts from the experiment described in Fig. 6A showed increased levels of activated caspase-8, caspase-9, caspase-3, cleaved PARP, and DR4 and decreased levels of CD44, RHAMM, HAS2, and caveolin-1 in tumor extracts from 4-MU–treated animals. This suggests that 4-MU reduces tumor growth by increasing apoptosis and decreasing the expression of HA receptors and related molecules.

Figure 6D shows decreased HA production in tumor-associated stroma and tumor cells in the specimen from 4-MU–treated animals when compared with vehicle-treated animals. As shown in Fig. 6D, a tumor specimen from the 4-MU–treated group had lower MVD than the vehicle-treated tumor. MVD (mean ± SD) in tumors from 4-MU–treated animals was 3.3-fold lower (10.8 ± 4.3) than in the vehicle-treated animals (33.4 ± 9.1; $P < 0.001$). Because MVD was calculated as the number of microvessels per high power field, the observed decrease in MVD was most likely independent of tumor size or volume. On the contrary, an increase in TUNEL-positive cells was observed in tumor specimens from 4-MU–treated animals when compared with vehicle-treated animals (Fig. 6D). The apoptosis index in tumor specimens from the 4-MU–treated group was five times higher (61.4 ± 17.1) when compared with the vehicle-treated group (12.8 ± 7.7; $P < 0.001$).

Taxotere is approved for the treatment of castration-resistant prostate cancer. In PC3-ML xenograft models, a 20 mg/kg weekly dose of taxotere has been shown to cause 62% inhibition of tumor growth (44). Therefore, we examined whether the combination of 4-MU and taxotere might be more effective in inhibiting PC3-ML cell proliferation than individual treatments alone. As shown in Supplementary Fig. S4, 4-MU enhanced the cytotoxicity of docetaxel at each dose. At each 4-MU concentration with fixed taxotere concentration or at taxotere concentration with fixed 4-MU concentration, the growth inhibition caused by the combination was higher than each individual drug ($P < 0.01$ to $P < 0.0001$; Bonferroni multiple comparison test).

Discussion

In this study, we show that 4-MU, a dietary supplement and a HA synthesis inhibitor, is a potent apoptotic agent with strong anti-invasive and antiangiogenic properties against prostate cancer cells. Because 4-MU inhibits HA synthesis primarily by depleting UGA and the K_m of UGA-transferase and HA synthases is 100 to 200 μmol/L (35–37), the IC_{50} of 4-MU for inhibition of HA synthesis is in a high micromolar range. 4-MU is a small molecular weight compound (198 daltons) and has been used as a choleretic agent in clinical trials for hepatitis B and C at a 2.2 g/d dose (ClinicalTrials.gov identifier, NCT00225537). Therefore, administration of 4-MU at high micromolecular concentrations is feasible.

4-MU is a strong inducer of apoptosis in prostate cancer cells. Furthermore, the IC_{50}s for HA synthesis inhibition and induction of apoptosis (0.4 mmol/L) are the same in all five prostate cancer cell lines, regardless of their androgen sensitivity. Because addition of HA prevents the inhibitory effects of 4-MU on cell proliferation and apoptosis, it indicates that 4-MU induces such effects by inhibiting HA synthesis. Upregulation of Fas-L, Fas, DR4, and FADD by 4-MU suggests that apoptosis induction by 4-MU involves the death receptor pathway. We have previously reported that HAS1 knockdown increases Fas and FADD expression, and transcriptionally downregulates CD44 (16). CD44 has been shown to regulate death receptor–mediated apoptosis (45). However, 4-MU also induces apoptosis in cell lines which do not express CD44 (e.g., LNCaP and LAPC-4; ref. 46). All prostate cancer cell lines used in this study express RHAMM (unpublished results). RHAMM-HA interaction also induces phosphoinositide 3-kinase signaling, which in turn, promotes survival by downregulating Fas and death receptor signaling (47). The data in Figs. 3D and 4B show that the addition of HA prevented the 4-MU–induced downregulation of CD44 and RHAMM both at the protein and mRNA levels. The availability of HA receptors might explain why the addition of HA is able to prevent 4-MU–induced apoptosis and motility in a significant manner.

Phosphoinositide 3-kinase/Akt signaling is known to promote survival by downregulating Fas and death receptor signaling (48). Because myr-Akt expression prevents the effects of 4-MU on cell growth, apoptosis, and gene expression, it indicates that inhibition of Akt signaling is an important mechanism in the antitumor activity of 4-MU. NF-κB activation induces the expression of chemokines and chemokine receptors (25–30). Akt signaling regulates CXCR4, which may regulate CXCR7, and CD44 may be a downstream target of CXCR7 (49). Because HA either completely or partially

prevents the 4-MU–induced decrease in CXCR1, CXCR4, CXCR-7, and IL-8 expression, the inhibitory effect of 4-MU on the expression of these genes is likely through the inhibition of HA synthesis. 4-MU is a strong inhibitor of caveolin-1 expression; however, this inhibition is independent of the inhibitory effect of 4-MU on HA synthesis and subsequent Akt activation.

Our data show that 4-MU inhibits tumor growth in the PC3-ML xenograft model. Because HA increases hydration and opens up spaces in tissues, it is possible that the observed decrease in tumor volumes in 4-MU–treated animals is not due to decreased tumor burden. However, the tumor weight in 4-MU–treated animals was four times lower than in the vehicle-treated animals. HA is present in tumor tissues in microgram amounts (50), and therefore, the decrease in the amount of HA (and consequently, decreased water content) due to 4-MU treatment cannot possibly account for the decrease in tumor weight which was in milligrams. Furthermore, the increased apoptosis index in 4-MU–treated tumors supports the notion that the decrease in tumor volume/weight observed in 4-MU–treated tumors was due to smaller tumor burden.

The trend observed in cell culture studies regarding downregulation of CD44, RHAMM, HAS2, and caveolin-1 and upregulation of apoptosis signaling proteins is also present in 4-MU–treated tumor tissues. The decrease in RHAMM and CD44 in 4-MU–treated tumor tissues (≥50%; Fig. 6) is less than the decrease observed in cell culture studies (≥80%). The differences observed in tumor specimens and cell culture experiments may be due to the fact that the observed CD44 and RHAMM levels in tumor tissue extracts are contributed by both tumor cells and stromal components. The effect of 4-MU on the latter is currently unknown.

Our study shows that 4-MU is a potent, orally bioavailable and relatively nontoxic anticancer agent with significant anti-invasive, antiangiogenic, and possibly, anti-inflammatory properties. Because 4-MU downregulates HA receptors, HAS2 and caveolin-1 expression and Akt signaling, it may be a better therapeutic approach than targeting individual HA receptors.

Disclosure of Potential Conflicts of Interest

No potential conflicts of interest were disclosed.

Acknowledgments

We thank Cynthia Soloway for critically reviewing the manuscript.

Grant Support

R01 CA 123063-03 (V.B. Lokeshwar) and R01CA72821-09 (V.B. Lokeshwar).
The costs of publication of this article were defrayed in part by the payment of page charges. This article must therefore be hereby marked *advertisement* in accordance with 18 U.S.C. Section 1734 solely to indicate this fact.

Received 08/25/2009; revised 01/06/2010; accepted 01/11/2010; published OnlineFirst 03/23/2010.

References

1. Volpi N, Schiller J, Stern R, Soltés L. Role, metabolism, chemical modifications and applications of hyaluronan. Curr Med Chem 2009;16:1718–45.
2. Ekici S, Cerwinka WH, Duncan R, et al. Comparison of the prognostic potential of hyaluronic acid, hyaluronidase (HYAL-1), CD44v6 and microvessel density for prostate cancer. Int J Cancer 2004;112:121–9.
3. Posey JT, Soloway MS, Ekici S, et al. Evaluation of the prognostic potential of hyaluronic acid and hyaluronidase (HYAL1) for prostate cancer. Cancer Res 2003;63:2638–44.
4. Aaltomaa S, Lipponen P, Tammi R, et al. Strong stromal hyaluronan expression is associated with PSA recurrence in local prostate cancer. Urol Int 2002;69:266–72.
5. Gomez CS, Gomez P, Knapp J, et al. Hyaluronic acid and HYAL-1 in prostate biopsy specimens: predictors of biochemical recurrence. J Urol 2009;182:1350–6.
6. Lokeshwar VB, Rubinowicz D, Schroeder GL, et al. Stromal and epithelial expression of tumor markers hyaluronic acid and HYAL1 hyaluronidase in prostate cancer. J Biol Chem 2001;276:11922–32.
7. Simpson MA, Lokeshwar VB. Hyaluronan and hyaluronidase in genitourinary tumors. Front Biosci 2008;13:5664–80.
8. Itano N, Atsumi F, Sawai T, et al. Abnormal accumulation of hyaluronan matrix diminishes contact inhibition of cell growth and promotes cell migration. Proc Natl Acad Sci U S A 2002;99:3609–14.
9. Kerbel RS, St Croix B, Florenes VA, Rak J. Induction and reversal of cell adhesion-dependent multicellular drug resistance in solid breast tumors. Hum Cell 1996;9:257–64.
10. Itano N, Sawai T, Yoshida M, et al. Three isoforms of mammalian hyaluronan synthases have distinct enzymatic properties. J Biol Chem 1999;274:25085–92.
11. Itano N, Sawai T, Atsumi F, et al. Selective expression and functional characteristics of three mammalian hyaluronan synthases in oncogenic malignant transformation. J Biol Chem 2004;279:18679–87.
12. Itano N, Kimata K. Altered hyaluronan biosynthesis in cancer progression. Semin Cancer Biol 2008;18:268–74.
13. Bharadwaj AG, Kovar JL, Loughman E, Elowsky C, Oakley GG, Simpson MA. Spontaneous metastasis of prostate cancer is promoted by excess hyaluronan synthesis and processing. Am J Pathol 2009;174:1027–36.
14. Bharadwaj AG, Rector K, Simpson MA. Inducible hyaluronan production reveals differential effects on prostate tumor cell growth and tumor angiogenesis. J Biol Chem 2007;282:20561–72.
15. Simpson MA, Wilson CM, McCarthy JB. Inhibition of prostate tumor cell hyaluronan synthesis impairs subcutaneous growth and vascularization in Immunocompromised mice. Am J Pathol 2002;161:849–57.
16. Golshani R, Lopez L, Estrella V, Kramer M, Iida N, Lokeshwar VB. Hyaluronic acid synthase-1 expression regulates bladder cancer growth, invasion, and angiogenesis through CD44. Cancer Res 2008;68:483–91.
17. Li Y, Li L, Brown TJ, Heldin P. Silencing of hyaluronan synthase 2 suppresses the malignant phenotype of invasive breast cancer cells. Int J Cancer 2007;120:2557–67.
18. Lokeshwar VB, Cerwinka WH, Isoyama T, Lokeshwar BL. HYAL1 hyaluronidase in prostate cancer: a tumor promoter and suppressor. Cancer Res 2005;65:7782–9.
19. Lokeshwar VB, Cerwinka WH, Lokeshwar BL. HYAL1 hyaluronidase: a molecular determinant of bladder tumor growth and invasion. Cancer Res 2005;65:2243–50.
20. Misra S, Toole BP, Ghatak S. Hyaluronan constitutively regulates activation of multiple receptor tyrosine kinases in epithelial and carcinoma cells. J Biol Chem 2006;281:34936–41.

21. Ghatak S, Misra S, Toole BP. Hyaluronan constitutively regulates ErbB2 phosphorylation and signaling complex formation in carcinoma cells. J Biol Chem 2005;280:8875–83.
22. Bourguignon LY, Spevak CC, Wong G, Xia W, Gilad E. Hyaluronan-CD44 Interaction with PKC-epsilon promotes oncogenic signaling by the stem cell marker, Nanog and the production of microRNA-21 leading to downregulation of the tumor suppressor protein, PDCD4, anti-apoptosis and chemotherapy resistance in breast tumor cells. J Biol Chem 2009;284:26533–46.
23. Kim Y, Lee YS, Choe J, Lee H, Kim YM, Jeoung D. CD44-epidermal growth factor receptor interaction mediates hyaluronic acid-promoted cell motility by activating protein kinase C signaling involving Akt, Rac1, Phox, reactive oxygen species, focal adhesion kinase, and MMP-2. J Biol Chem 2008;283:22513–28.
24. Murray D, Morrin M, McDonnell S. Increased invasion and expression of MMP-9 in human colorectal cell lines by a CD44-dependent mechanism. Anticancer Res 2004;24:489–94.
25. Desai B, Rogers MJ, Chellaiah MA. Mechanisms of osteopontin and CD44 as metastatic principles in prostate cancer cells. Mol Cancer 2007;6:18.
26. Horton MR, Boodoo S, Powell JD. NF-κB activation mediates the cross-talk between extracellular matrix and interferon-gamma (IFN-γ) leading to enhanced monokine induced by IFN-gamma (MIG) expression in macrophages. J Biol Chem 2002;277:43757–62.
27. Voelcker V, Gebhardt C, Averbeck M, et al. Hyaluronan fragments induce cytokine and metalloprotease upregulation in human melanoma cells in part by signalling via TLR4. Exp Dermatol 2008;17:100–7.
28. Mascarenhas MM, Day RM, Ochoa CD, et al. Low molecular weight hyaluronan from stretched lung enhances interleukin-8 expression. Am J Respir Cell Mol Biol 2004;30:51–60.
29. Tonnarelli B, Manferdini C, Piacentini A, et al. Surface-dependent modulation of proliferation, bone matrix molecules, and inflammatory factors in human osteoblasts. J Biomed Mater Res A 2009;89: 687–96.
30. Lisignoli G, Cristino S, Piacentini A, Cavallo C, Caplan AI, Facchini A. Hyaluronan-based polymer scaffold modulates the expression of inflammatory and degradative factors in mesenchymal stem cells: involvement of Cd44 and Cd54. J Cell Physiol 2006;207:364–73.
31. Araki S, Omori Y, Lyn D, et al. Interleukin-8 is a molecular determinant of androgen independence and progression in prostate cancer. Cancer Res 2007;67:6854–62.
32. Rilla K, Pasonen-Seppanen S, Rieppo J, Tammi M, Tammi R. The hyaluronan synthesis inhibitor 4-methylumbelliferone prevents keratinocyte activation and epidermal hyperproliferation induced by epidermal growth factor. J Invest Dermatol 2004;123:708–14.
33. Kudo D, Kon A, Yoshihara S, et al. Effect of a hyaluronan synthase suppressor, 4-methylumbelliferone, on B16F-10 melanoma cell adhesion and locomotion. Biochem Biophys Res Commun 2004; 321:783–7.
34. Yoshihara S, Kon A, Kudo D, et al. A hyaluronan synthase suppressor, 4-methylumbelliferone, inhibits liver metastasis of melanoma cells. FEBS Lett 2005;579:2722–6.
35. Kakizaki I, Kojima K, Takagaki K, et al. A novel mechanism for the inhibition of hyaluronan biosynthesis by 4-methylumbelliferone. J Biol Chem 2004;279:33281–9.
36. Kakizaki I, Takagaki K, Endo Y, et al. Inhibition of hyaluronan synthesis in *Streptococcus equi* FM100 by 4-methylumbelliferone. Eur J Biochem 2002;269:5066–75.
37. Morohashi H, Kon A, Nakai M, et al. Study of hyaluronan synthase inhibitor, 4-methylumbelliferone derivatives on human pancreatic cancer cell (KP1-NL). Biochem Biophys Res Commun 2006;345: 1454–9.
38. Kultti A, Pasonen-Seppänen S, Jauhiainen M, et al. 4-Methylumbelliferone inhibits hyaluronan synthesis by depletion of cellular UDP-glucuronic acid and downregulation of hyaluronan synthase 2 and 3. Exp Cell Res 2009;315:1914–23.
39. Lokeshwar VB, Estrella V, Lopez L, et al. HYAL1–1, an alternatively spliced variant of HYAL1 hyaluronidase: a negative regulator of bladder cancer. Cancer Res 2006;66:11219–27.
40. Lokeshwar VB, Gomez P, Kramer M, et al. Epigenetic regulation of HYAL-1 hyaluronidase expression. Identification of HYAL-1 promoter. J Biol Chem 2008;283:29215–27.
41. Lokeshwar BL, Lokeshwar VB, Block NL. Expression of CD44 in prostate cancer cells: association with cell proliferation and invasive potential. Anticancer Res 1995;15:1191–8.
42. Thompson TC, Tahir SA, Li L, et al. The role of caveolin-1 in prostate cancer: clinical implications. Prostate Cancer Prostatic Dis 2009;13: 6–11.
43. Omarbasha B, Fair WR, Heston WD. Effect of coumarin on the normal rat prostate and on the R-3327H prostatic adenocarcinoma. Cancer Res 1989;49:3045–9.
44. Liu G, Taylor SA, Marrinan CH, et al. Continuous and intermittent dosing of lonafarnib potentiates the therapeutic efficacy of docetaxel on preclinical human prostate cancer models. Int J Cancer 2009;125: 2711–20.
45. Hauptschein RS, Sloan KE, Torella C, et al. Functional proteomic screen identifies a modulating role for CD44 in death receptor-mediated apoptosis. Cancer Res 2005;65:1887–96.
46. Freedland SJ, Seligson DB, Liu AY, et al. Loss of CD10 (neutral endopeptidase) is a frequent and early event in human prostate cancer. Prostate 2003;55:71–80.
47. Gouëffic Y, Guilluy C, Guérin P, Patra P, Pacaud P, Loirand G. Hyaluronan induces vascular smooth muscle cell migration through RHAMM-mediated PI3K-dependent Rac activation. Cardiovasc Res 2006;72:339–48.
48. Kim MJ, Kim HB, Bae JH, et al. Sensitization of human K562 leukemic cells to TRAIL-induced apoptosis by inhibiting the DNA-PKcs/Akt-mediated cell survival pathway. Biochem Pharmacol 2009;78: 573–82.
49. Wang J, Shiozawa Y, Wang J, et al. The role of CXCR7/RDC1 as a chemokine receptor for CXCL12/SDF-1 in prostate cancer. J Biol Chem 2008;283:4283–94.
50. Lokeshwar VB, Obek C, Soloway MS, Block NL. Tumor-associated hyaluronic acid: a new sensitive and specific urine marker for bladder cancer. Cancer Res 1997;57:773–7, Erratum in: Cancer Res 1998;58:3191.